

Computing Smooth Approximations of Scalar Functions with Constraints

Giuseppe Patanè^a, Bianca Falcidieno^a

^a*Istituto di Matematica Applicata e Tecnologie Informatiche - Consiglio Nazionale delle Ricerche, Genova, Italy*

Abstract

In engineering, geographical applications, scientific visualization, and bio-informatics, a variety of phenomena is described by a large set of data modeled as the values of a scalar function $f : \mathcal{M} \rightarrow \mathbb{R}$ defined on a surface \mathcal{M} . A low quality of the discrete representations of the input data, unstable computations, numerical approximations, and noise might produce functions with a high number of critical points. In this context, we propose an algorithmic framework for smoothing an arbitrary scalar function, while simplifying its redundant critical points and preserving those that are mandatory for its description. From our perspective, the critical points of f are a natural choice to guide the approximation scheme; infact, they usually represent relevant information about the behavior of f or the shape itself. To address the aforementioned aims, we compute a smooth approximation $\tilde{f} : \mathcal{M} \rightarrow \mathbb{R}$ of f whose set of critical points contains those that have been preserved by the simplification process. The idea behind the proposed approach is to combine smoothing techniques, critical points, and spectral properties of the Laplacian matrix. Inserting constraints in the smoothing of f allows us to overcome the traditional error-driven approximation of f , which does not provide constraints on the preserved topological features. Finally, the computational cost of the proposed approach is $O(n \log n)$, where n is the number of vertices of \mathcal{M} .

Key words: Signal and function smoothing, critical points, Laplacian matrix, shape analysis, Morse complex, level sets.

1. Introduction

Scalar functions are extensively used to model data in engineering, geographical applications, scientific visualization, and bio-informatics. In each of these research fields, a variety of phenomena is described by a large set of data modeled as the values of a scalar function defined on a surface. These values can be acquired from the real world (e.g., terrain models in GIS) or generated by solving simulation problems (e.g., fluid dynamics, heat equation [3, 18]).

In the aforementioned contexts, an arbitrary scalar function $f : \mathcal{M} \rightarrow \mathbb{R}$, defined on a 2-manifold surface \mathcal{M} , is usually associated to a high differential noise, which is due to a low quality of the discrete representations of the input data, unstable computations, and numerical approximations. Here, as *differential noise* of f we refer to a high number of critical points, which have very close positions or f -values, include multiple saddles, and generally do not verify the Euler formula. From our perspective, the critical points of f are a natural choice to guide the approximation and smoothing of f ; infact, they usually represent relevant information about its behavior. Computing and controlling the distribution of the critical points of smooth approximations of noisy maps is also crucial for quadrilateral remeshing [8, 18], shape [6, 9, 10] and molecular [17] analysis. In the following, as (discrete) smooth approximation of f we refer to any approximation of f with regular (i.e., un-noisy) level sets and a generally low number of non-clustered critical points.

In the literature (see Section 2.2), there are two main approaches to discarding irrelevant critical points. The former is to cancel pairs of critical points [6, 9, 10], relying on their topological structures as captured by the Morse complex. At the end of the procedure, the Morse complex is no more associated to a corresponding scalar function. The latter works in the function space and applies isotropic Laplacian filters [8, 18, 24] or bilateral smoothing operators to the function itself [15]. Here, the main drawback of these techniques is the lack of control on the final number and distribution of the critical points of the smoothed function, which also depend on the number of times the filter has been applied.

In this context, we present a novel framework for simplifying the critical points of a noisy scalar function $f : \mathcal{M} \rightarrow \mathbb{R}$ and computing a smooth approximation $\tilde{f} : \mathcal{M} \rightarrow \mathbb{R}$ of f constrained to the f -values at a set \mathcal{C} of *feature points* for f . The set \mathcal{C} is defined by evaluating the significance of the critical points through a novel simplification procedure, which considers the variation of the f -values on \mathcal{M} . Then, we compute a smooth approximation \tilde{f} of f using the f -values at \mathcal{C} as interpolating or least-squares constraints. Finally, the computational cost of the proposed framework is $O(n \log n)$, where n is the number of vertices of \mathcal{M} .

Even though we mainly use the critical points of f to guide its smoothing and approximation, other choices of the set of feature points are possible without changing the overall structure of the proposed approach. For instance, the feature points can be defined through the analysis of the f -values based on clustering techniques (e.g., principal component analysis, k -means clustering) or guided by *a-priori* information on f or the appli-

Email addresses: patane@ge.imati.cnr.it (Giuseppe Patanè),
falcidieno@ge.imati.cnr.it (Bianca Falcidieno)

cation context.

The idea behind our approach is to combine the least-squares approximation [12] and *Tikhonov regularization* [4, 26] with the smoothing and spectral properties of the Laplace-Beltrami operator. By adapting Tikhonov regularization to the case of scalar functions defined on surfaces, we introduce an unconstrained smoothing algorithm based on the minimization of a functional \mathcal{F} . Here, \mathcal{F} is a trade-off between approximation accuracy and smoothness of the solution. This choice also allows us to easily insert constraints in the smoothing process and to control the number of preserved critical points. The constrained and unconstrained smoothing reduces to solving a sparse linear system with direct or iterative techniques [12]. In case of interpolating constraints, the set of critical points of \tilde{f} contains \mathcal{C} plus a number of additional and well-behaved maxima, minima, and saddles, which is low with respect to those of f .

With our approach, the points of \mathcal{C} are preserved in \tilde{f} without diffusing them. On the contrary, the isotropy of the Laplacian matrix indiscriminately smooths noise and topological features [8, 18, 24] without constraints on their relocations or cancellations. Constrained least-squares techniques [22] have been efficiently used to define compression schemes based on the selection of a set of anchors. While in [22] the choice of the constrained vertices is guided by the final approximation accuracy of the reconstructed surface, in this work the emphasis is on the preservation of the differential properties of f through the simplification of its critical points. Figure 1 gives an overview of the proposed approach.

The paper is organized as follows: in Section 2, we introduce the theoretical background on the representation and differential analysis of an arbitrary scalar function f defined on triangulated surfaces. Section 3 introduces a novel method to robustly classify and simplify the critical points of f . In Section 4, we describe two approaches to smoothing a scalar function using interpolating or least-squares constraints. Section 5 discusses the main properties of the proposed approach and Section 6 concludes the paper.

2. Related work

We briefly introduce the theoretical background on the triangle-based representation (see Section 2.1), simplification and smoothing (see Section 2.2) of scalar functions defined on triangulated surfaces.

2.1. Discrete scalar functions defined on triangulated surfaces

We represent a 2-manifold surface as a triangle mesh $\mathcal{M} := (P, T)$ where $P := \{\mathbf{p}_i, i = 1, \dots, n\}$ is a set of n vertices and T is an *abstract simplicial complex* that contains the adjacency information about \mathcal{M} . The piecewise linear function $f : \mathcal{M} \rightarrow \mathbb{R}$ is defined by linearly interpolating the values $(f(\mathbf{p}_i))_{i=1}^n$ of f at the vertices by using barycentric coordinates. Finally, we assume that f is a *general* scalar function; that is, $f(\mathbf{p}_i) \neq f(\mathbf{p}_j)$, for each edge (i, j) of \mathcal{M} .

The analysis of $f : \mathcal{M} \rightarrow \mathbb{R}$ is usually based on the study of its level sets $\gamma_\alpha := \{\mathbf{p} \in \mathcal{M} : f(\mathbf{p}) = \alpha\}$; as α varies, the behavior of f is mainly conveyed by the critical points of f at

which the level sets split, merge, and join. In the following, we refer to the critical points of f as the *topological features* of f . Assuming that f is general, the critical points of f occur only at the mesh vertices. These points correspond to the maxima, minima, and saddles of f and are computed by analyzing the distribution of the f -values on the neighborhoods of each vertex [2]. For more details on the computation of the critical points, we refer the reader to [5] and Section 3.

Since the critical points and shape of the level sets are independent of positive re-scalings of the function values, we assume that the values of the piecewise linear function f have been normalized in such a way that $\text{Image}(f) := \{f(\mathbf{p}), \mathbf{p} \in \mathcal{M}\}$ is the interval $[0, 1]$. Among several error metrics, we use the L_∞ -error between two functions $f_1, f_2 : \mathcal{M} \rightarrow \mathbb{R}$, which is defined as $\|f_1 - f_2\|_\infty := \max_{i=1, \dots, n} \{|f_1(\mathbf{p}_i) - f_2(\mathbf{p}_i)|\}$.

2.2. Simplification and smoothing of scalar functions

Given a scalar function f with a large number of critical points associated to a low variation of the f -values, [6] defines a topological hierarchy for f that is constructed by performing a progressive simplification of the Morse complex \mathcal{F} of f through the cancellation of pairs of critical points. Then, the critical points are paired by visiting \mathcal{M} with respect to the reordering of its vertices according to increasing values of f . The importance weight associated to the pair $(\mathbf{p}_i, \mathbf{p}_j)$ is measured as the *persistence* of $\mathbf{p}_i, \mathbf{p}_j$, that is, $|f(\mathbf{p}_i) - f(\mathbf{p}_j)|$. The local updates of the complex are performed by iteratively removing those pairs with the lowest persistence and reconnecting the neighbors of the removed nodes. Each node removal affects the number and configuration of the critical points of \mathcal{F} without changing f . Therefore, the simplification provides a hierarchy for f where each Morse complex $\mathcal{F}^{(k)}$ is not associated to a corresponding scalar function $f^{(k)}$ on \mathcal{M} .

Recently, [10] has proposed a technique that replaces f with a new function \tilde{f} that has the same points of persistency of f higher than a given threshold ϵ and the L_∞ -error between f and \tilde{f} is lower than ϵ . The ϵ -*simplification* of the structure of f and the construction of \tilde{f} are based on an iterative process, which cancels minimum-saddle pairs by sweeping the vertices from bottom to top and lower the saddles that belong to a pair of persistency lower than ϵ .

An alternative way is to consider a polynomial *transfer function* φ and define the *Laplacian low-pass filter* $\mathbf{f} \rightarrow \varphi(L)\mathbf{f}$ [18, 24]. Here, $L \in \mathbb{R}^{n \times n}$ is the Laplacian matrix associated to \mathcal{M} and $\mathbf{f} := (f(\mathbf{p}_i))_{i=1}^n \in \mathbb{R}^{n \times 1}$ is the vector of function values at the mesh vertices (see Section 4.1). Small powers of L attenuate higher frequencies of f and the definition of the Laplacian filter resembles the convolution operator.

Finally, [15] introduces a bilateral filter operator, which updates $f(\mathbf{p}_i)$ using a weighted average $s_\sigma(\mathbf{p}_i)$ of the function differences between its neighboring vertices and \mathbf{p}_i . For $i = 1, \dots, n$, this value is defined as

$$s_\sigma(\mathbf{p}_i) := \frac{\sum_{\mathbf{p}_j \in \mathcal{N}(\mathbf{p}_i, \sigma)} f_{ij} \varphi_{\sigma_1}(d_{ij}) \varphi_{\sigma_2}(f_{ij})}{\sum_{\mathbf{p}_j \in \mathcal{N}(\mathbf{p}_i, \sigma)} \varphi_{\sigma_1}(d_{ij}) \varphi_{\sigma_2}(f_{ij})},$$

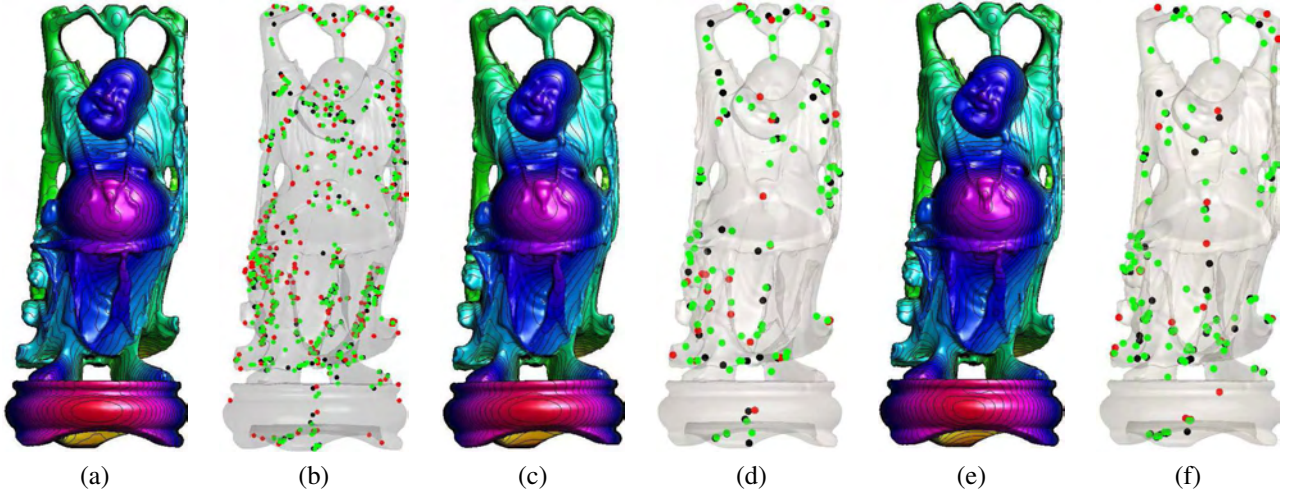


Figure 1: Level sets and critical points (a,b) of an input scalar function ($m = 174$, $M = 180$, $s = 370$) and its smoothed version achieved by applying the Tikhonov regularization without (c,d) ($m = 44$, $M = 31$, $s = 91$) and (e,f) with ($m = 65$, $M = 23$, $s = 104$) least-squares constraints. In both cases, the L_∞ -approximation error is lower than 1%. Red, black, and green points locate the m minima, M maxima, and s saddle points of the corresponding function.

with weights $d_{ij} := \|\mathbf{p}_j - \mathbf{p}_i\|_2$ and $f_{ij} := |f(\mathbf{p}_j) - f(\mathbf{p}_i)|$. The function $\varphi_\sigma(t) := e^{-\frac{t^2}{2\sigma}}$ is the Gaussian kernel of support σ and $\mathcal{N}(\mathbf{p}_i, \sigma)$ is the set of vertices of \mathcal{M} that fall inside the sphere of center \mathbf{p}_i and radius σ . Once the value $s_\sigma(\mathbf{p}_i)$ has been computed, each function value $f(\mathbf{p}_i)$ is updated to $\tilde{f}(\mathbf{p}_i) := f(\mathbf{p}_i) + s_\sigma(\mathbf{p}_i)$ and the iteration proceeds until a chosen number k of steps is reached. This approach requires to set the parameters σ_1 , σ_2 , σ , k and does not have a direct control on the final number of preserved critical points. The methods in [9, 10, 15] take $O(n \log n)$ -time and [24] is linear in the number n of vertices of \mathcal{M} .

3. Simplifying the critical points of scalar functions

In the following, we introduce a novel method to robustly classify and simplify the critical points of a function $f: \mathcal{M} \rightarrow \mathbb{R}$. The idea behind our simplification of the critical points is to modify the definition in [2], which classifies the vertices of \mathcal{M} on the base of the distribution of the f -values on their local neighborhoods. We propose to check the changes of the sign of f along the edges of the 1-star of each vertex with respect to a positive threshold δ . Indeed, the δ -sensitive sign of f along the oriented edge $(\mathbf{p}_i, \mathbf{p}_j)$ is defined as positive if $f(\mathbf{p}_j) - f(\mathbf{p}_i) > \delta$; in this case, we write $f(\mathbf{p}_j) >_\delta f(\mathbf{p}_i)$. Similarly, the δ -sensitive sign of f along the previous edge is considered as negative if $f(\mathbf{p}_j) - f(\mathbf{p}_i) < -\delta$; hence, we write $f(\mathbf{p}_j) <_\delta f(\mathbf{p}_i)$. Formally, if we let

$$Lk(i) := \{j_1, \dots, j_k \in N(i) : (j_l, j_{l+1})_{s=1}^k \text{ edges of } \mathcal{M}\}$$

be the *link* of i , then the (δ -sensitive) *upper link* is defined as

$$Lk^+(i) := \{j_l \in Lk(i) : f(\mathbf{p}_{j_l}) >_\delta f(\mathbf{p}_i)\},$$

and the (δ -sensitive) *mixed link* as

$$Lk^\pm(i) := \{j_l \in Lk(i) : f(\mathbf{p}_{j_{l+1}}) >_\delta f(\mathbf{p}_i) >_\delta f(\mathbf{p}_{j_l}) \text{ or } f(\mathbf{p}_{j_{l+1}}) <_\delta f(\mathbf{p}_i) <_\delta f(\mathbf{p}_{j_l})\},$$

where $j_{k+1} := j_1$. For the definition of the *lower link*, we replace the inequality “ $>_\delta$ ” with “ $<_\delta$ ” in the definition of the upper link. If $Lk^+(i) = \emptyset$ or $Lk^-(i) = \emptyset$, then \mathbf{p}_i is a δ -sensitive *maximum* or *minimum*, respectively. If the cardinality of the set $Lk^\pm(i)$ is $2 + 2m_i$, then \mathbf{p}_i is classified as a *saddle of multiplicity* $m_i \geq 1$. We note that if $\delta = 0$, then we get the definition introduced in [2]. Under the assumption that \mathcal{M} is a closed surface and $\delta = 0$, the *Euler formula*

$$\chi(\mathcal{M}) = m - s + M, \quad g = \frac{1}{2}(2 - \chi(\mathcal{M})),$$

gives the link between the critical points of (\mathcal{M}, f) and the Euler characteristic $\chi(\mathcal{M})$ of \mathcal{M} [2, 16]. Here, m and M is the number of minima and maxima; the $s := \sum_{\mathbf{p}_i \text{ saddle}} m_i$ saddle points of f are counted with their multiplicity m_i . If δ is not null, then the preserved critical points no necessarily satisfy the Euler formula. Indicating with \mathcal{C}_δ the critical points of f that are preserved after the simplification with respect to δ , we get that $\delta > \delta'$ implies $\mathcal{C}_\delta \subseteq \mathcal{C}_{\delta'}$ and the set $\{\mathcal{C}_\delta\}_\delta$ gives a hierarchy of simplified critical points. Increasing δ , a larger number of critical points of f is simplified. In our implementation, the parameter δ is proportional to the maximum variation $\max_{(i,j) \text{ edge}} \{|f(\mathbf{p}_i) - f(\mathbf{p}_j)|\}$ of the f -values along the edges of \mathcal{M} . Note that the computational cost of the simplification procedure is $O(n)$, where n is the number of vertices. Infact, we need to visit all the 1-stars of \mathcal{M} and compare the f -values along their edges. Examples of simplification of the critical points are shown in Figure 2 and 3.

4. Smoothing scalar functions

This section describes two approaches to smooth a scalar function f through the properties of the Laplace-Beltrami operator (see Section 4.1). The first one uses the Tikhonov regularization to smooth arbitrary signals and treat all the function values with the same degree of importance (see Section 4.2).

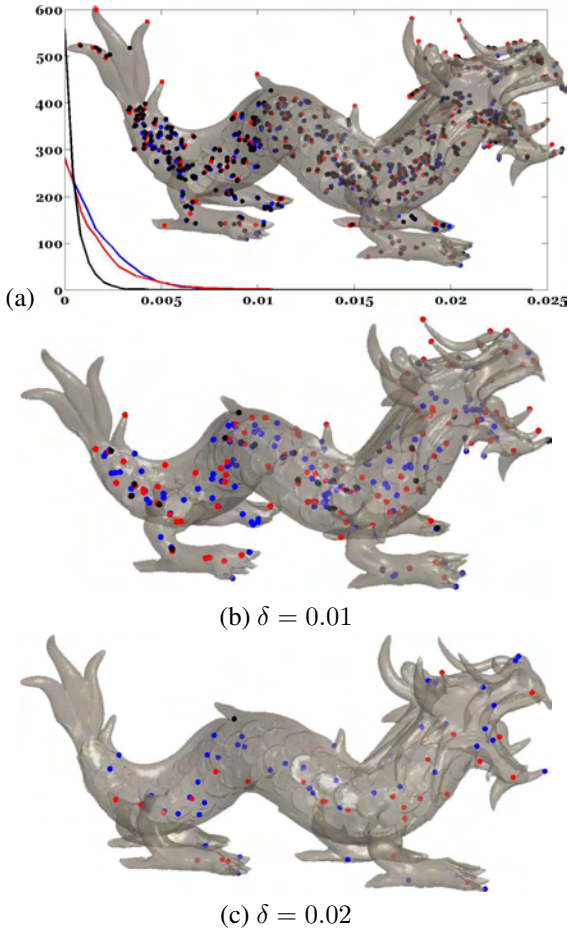


Figure 2: Simplification of the critical points with respect to a given threshold δ . (a) Evolution of the number of critical points (y -axis) with respect to a different threshold δ (x -axis): red, blue, and black curves represent the number of maxima, minima, and saddle points at each step. (b,c) Critical points preserved by the simplification.

We also replace the least-squares error of the Tikhonov regularization measured by the Euclidean norm with a metric induced by the geometry of the input surface. The second approach (see Section 4.3) computes a smooth approximation of f constrained to interpolate or approximate the values attained at a set \mathcal{C} of feature points. As \mathcal{C} , we consider all the critical points of f or those that are preserved by the δ -simplification. Finally, we analyze the approximation error between the input and the smoothed function.

4.1. Smoothing operators for scalar functions

The smoothness of a scalar function $f : \mathcal{M} \rightarrow \mathbb{R}$ is defined by imposing that the value of f at a vertex differs as little as possible from the f -values on its neighbors. Therefore, a smoothing operator [24] assigns to each value $f(\mathbf{p}_i)$ the difference between $f(\mathbf{p}_i)$ and the weighted average of its neighbors, that is,

$$f(\mathbf{p}_i) - \frac{\sum_{j \in N(i)} w_{ij} f(\mathbf{p}_j)}{\sum_{j \in N(i)} w_{ij}}, \quad i = 1, \dots, n,$$

with w_{ij} real weight. The 1-star of \mathbf{p}_i is defined as the set $N(i) := \{j : (i, j) \text{ edge}\}$ of the vertices adjacent to i . The co-

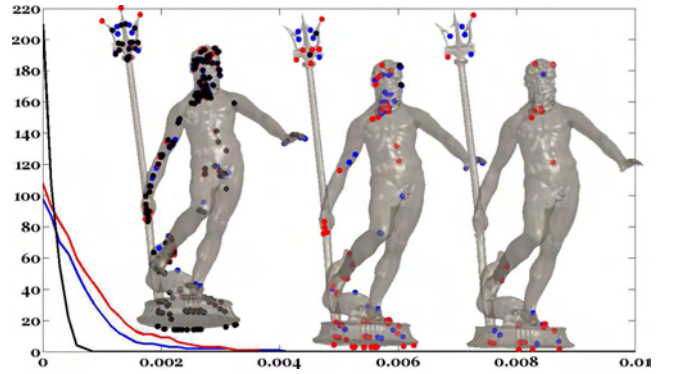


Figure 3: Simplification of the critical points with respect to a different threshold (x -axis), which increases from left to right; the initial set of critical points is shown in the left image.

efficients w_{ij} have been computed by minimizing the Dirichlet energy [7, 19] and the mean-value theorem [11]. In our tests, we used $w_{ij} := (\cot \alpha_{ij} + \cot \beta_{ij})/2$ [19], where α_{ij}, β_{ij} are the angles opposite to the edge (i, j) . These weights give a sparse and symmetric Laplacian matrix; finally, the mean-value [11] and normalized cotangent weights [7] are possible alternatives. Indicating with $\mathbf{f} := (f(\mathbf{p}_i))_{i=1}^n \in \mathbb{R}^{n \times 1}$ the array of the f -values at the mesh vertices of \mathcal{M} , the Laplace-Beltrami operator can be approximated as $\mathbf{f} \rightarrow L\mathbf{f}$, where $L := (l_{ij})_{ij} \in \mathbb{R}^{n \times n}$

$$l_{ij} := \begin{cases} \sum_{k \neq i} w_{ik} & i = j, \\ -w_{ij} & (i, j) \text{ edge}, \\ 0 & \text{else,} \end{cases}$$

is the *graph Laplacian matrix*. For more details on the Laplacian matrix and its applications, we refer the reader to surveys on mesh filtering [25], differential coordinates [21, 23], spectral methods [29] for mesh processing and shape analysis. Since $f = \text{const}$ implies that $\mathcal{S}(f) := \langle \mathbf{f}, L\mathbf{f} \rangle_2 := \mathbf{f}^T L\mathbf{f} = 0$, the value $\mathcal{S}(f)$ provides a measure of the smoothness of f . In fact, if $\mathcal{S}(f) \approx 0$ then the deviation of the f -values at each vertex from the average of its neighboring values is negligible. We refer to $\mathcal{S}(f)$ as the *Sobolev semi-norm* of f .

4.2. Smoothing scalar functions via Tikhonov regularization

Let $K : \mathcal{H} \rightarrow \mathbb{R}$ be an operator defined on a linear space \mathcal{H} of functions, e.g. the space of square-integrable functions on a 2-manifold or a Reproducing Kernel Hilbert Space [1]. Tikhonov regularization [4, 26] is commonly used to transform the ill-posed problem $Kf = g$, $f \in \mathcal{H}$, in a well-posed one; to this end, the regularized solution is computed by minimizing the functional

$$\mathcal{F}(f) := \epsilon \|Kf - g\|_{\mathcal{H}}^2 + \|Lf\|_{\mathcal{H}}^2, \quad f \in \mathcal{H},$$

on the linear space \mathcal{H} . Here, L is a regularization operator (e.g., the derivatives of a given order) and ϵ is a positive constant which defines the trade-off between the approximation error $\|Kf - g\|_{\mathcal{H}}$ and the smoothness energy $\|Lf\|_{\mathcal{H}}$.

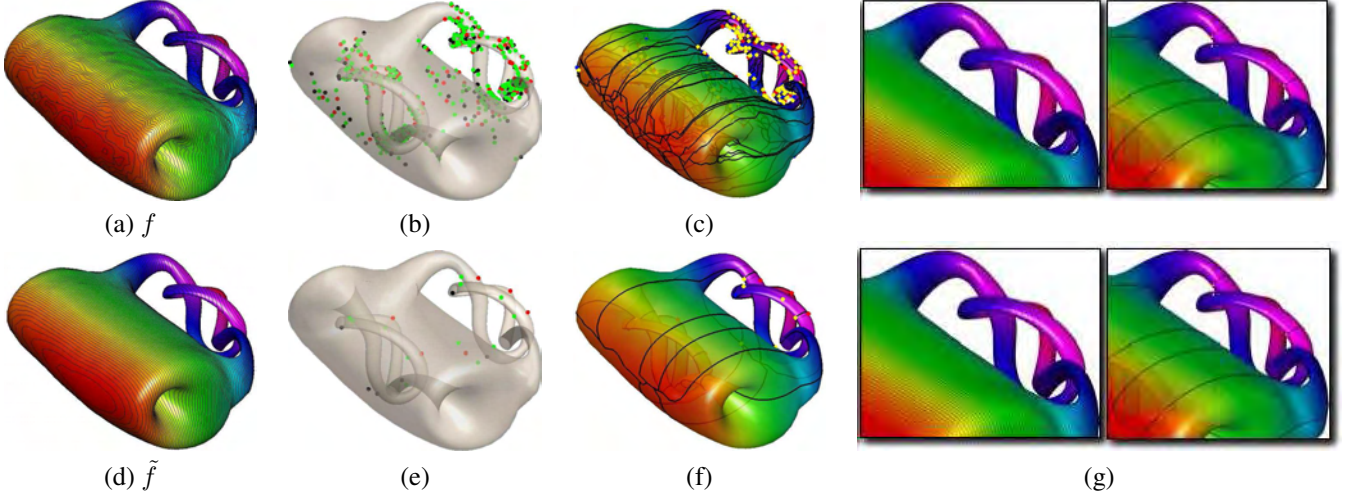


Figure 4: (a) Level sets, (b) critical points, and (c) Morse Complex of a scalar function f with $m = 28$ minima, $M = 28$ maxima, and $s = 58$ saddle points. The function f is smoothed using the Tikhonov regularization. (b) The smooth function \tilde{f} has $m = 6$, $M = 6$, and $s = 14$ critical points. The level sets, critical points, and Morse complex of \tilde{f} are shown in (d), (e), and (f). Comparing (c) with (f), we see that the paths of the Morse Complex have been smoothed. (g) Zoom-in on a handle of the input surface before and after the smoothing. The L_∞ -error between f and \tilde{f} is 0.087.

In the discrete setting, we apply the Tikhonov regularization to the scalar function $f : \mathcal{M} \rightarrow \mathbb{R}$, defined on a triangulated surface \mathcal{M} . Therefore, we replace f with the function $\tilde{f} : \mathcal{M} \rightarrow \mathbb{R}$, whose values $\tilde{\mathbf{f}} := (\tilde{f}(\mathbf{p}_i))_{i=1}^n \in \mathbb{R}^{n \times 1}$ at the mesh vertices minimize the functional

$$\mathcal{F}(\tilde{\mathbf{f}}) := \epsilon \|\tilde{\mathbf{f}} - \mathbf{f}\|_B^2 + \|\tilde{L}\tilde{\mathbf{f}}\|_2^2. \quad (1)$$

A natural choice of the smoothing operator L is the Laplacian matrix associated to \mathcal{M} . Therefore, $\mathcal{F}(\tilde{\mathbf{f}})$ is defined as the compromise between approximation accuracy $\|\tilde{\mathbf{f}} - \mathbf{f}\|_B$ and smoothness $\|\tilde{L}\tilde{\mathbf{f}}\|_2$ of the solution. The norm $\|\mathbf{x}\|_B^2 := \mathbf{x}^T B \mathbf{x}$ is induced by the scalar product $\langle \mathbf{x}, \mathbf{y} \rangle_B := \mathbf{x}^T B \mathbf{y}$, where B is a positive-definite matrix. Firstly, we consider the Euclidean distance (i.e., $B := I$). Then, we discuss a choice of B that takes into account the geometry of \mathcal{M} and is provided by the linear finite element discretization of the Laplace-Beltrami operator [20, 27].

Smoothing f using the Euclidean metric. Given $f : \mathcal{M} \rightarrow \mathbb{R}$, we apply the Tikhonov regularization [4, 26] and replace f with the function $\tilde{f} : \mathcal{M} \rightarrow \mathbb{R}$, whose values $\tilde{\mathbf{f}} := (\tilde{f}(\mathbf{p}_i))_{i=1}^n$ at the mesh vertices are defined as the solution of the following minimization problem (i.e., $B := I$ in (1))

$$\min_{\tilde{\mathbf{f}} \in \mathbb{R}^n} \{\epsilon \|\tilde{\mathbf{f}} - \mathbf{f}\|_2^2 + \|\tilde{L}\tilde{\mathbf{f}}\|_2^2\}. \quad (2)$$

The minimization problem (2) is equivalent to solve the *normal equation*

$$(L^T L + \epsilon I)\tilde{\mathbf{f}} = \epsilon \mathbf{f}; \quad (3)$$

the positive definitiveness of the coefficient matrix $(L^T L + \epsilon I)$ guarantees that $\tilde{\mathbf{f}}$ is unique (see Figure 4). Since the condition $N(i) \cap N(j) = \emptyset$ implies that $(L^T L)_{ij} = 0$, $i, j = 1, \dots, n$, the coefficient matrix in (3) is sparse and $\tilde{\mathbf{f}}$ can be efficiently computed through direct or iterative solvers of sparse linear systems [12].

Using the eigensystem of L , we express $\tilde{\mathbf{f}}$ as a linear combination of the eigenvectors of L and make explicit the regularization coefficients. More precisely, from the relations $L\mathbf{x}_i = \lambda_i \mathbf{x}_i$, $i = 1 \dots, n$, it follows that

$$LX = X\Delta, \quad \Delta := \text{diag}(\lambda_1, \dots, \lambda_n) \in \mathbb{R}^{n \times n},$$

with $X := [\mathbf{x}_1, \dots, \mathbf{x}_n] \in \text{Gl}_n(\mathbb{R})$ orthogonal matrix (i.e., $X^T X = I$). In the following, we assume that the eigenvalues of L have been reordered in increasing order, $0 = \lambda_1 \leq \dots, \leq \lambda_n$; finally, we remind that $\mathbf{x}_1 = \mathbf{1}$ is the constant eigenvector related to the eigenvalue $\lambda_1 = 0$. Applying this decomposition to the normal equation (3), we get the equivalent formulation $(\Delta^2 + \epsilon I)X^T \tilde{\mathbf{f}} = \epsilon X^T \mathbf{f}$ and the following representation of $\tilde{\mathbf{f}}$

$$\tilde{\mathbf{f}} = \sum_{i=1}^n \epsilon \frac{\mathbf{f}^T \mathbf{x}_i}{\lambda_i^2 + \epsilon} \mathbf{x}_i. \quad (4)$$

Assuming that the noise in f is concentrated in high frequency and the Fourier coefficient $|\mathbf{f}^T \mathbf{x}_i|$ decays rapidly with i , most of the energy of f can be reconstructed from the lowest frequency components \mathbf{x}_i and the noise contribution along \mathbf{x}_i is small. From equation (4), we conclude that the regularization term $(\lambda_i^2 + \epsilon)^{-1}$ filters out the contributions to the solution corresponding to the high eigenvalues (see Figure 5).

Smoothing f using the metric induced by the FEM discretization. For a triangulated surface \mathcal{M} , the basis functions $\{\mathbf{x}_i\}_{i=1}^n$ can also be computed solving the *generalized eigenvalue problem* [20, 27]

$$L\mathbf{x}_i = \lambda_i B \mathbf{x}_i, \quad i = 1, \dots, n, \quad 0 = \lambda_1 \leq \dots \leq \lambda_n,$$

where L is the *stiffness matrix* with cotangent weights and the *mass matrix* $B := (b_{ij})_{i,j=1}^n$ codes the geometry of \mathcal{M} in terms

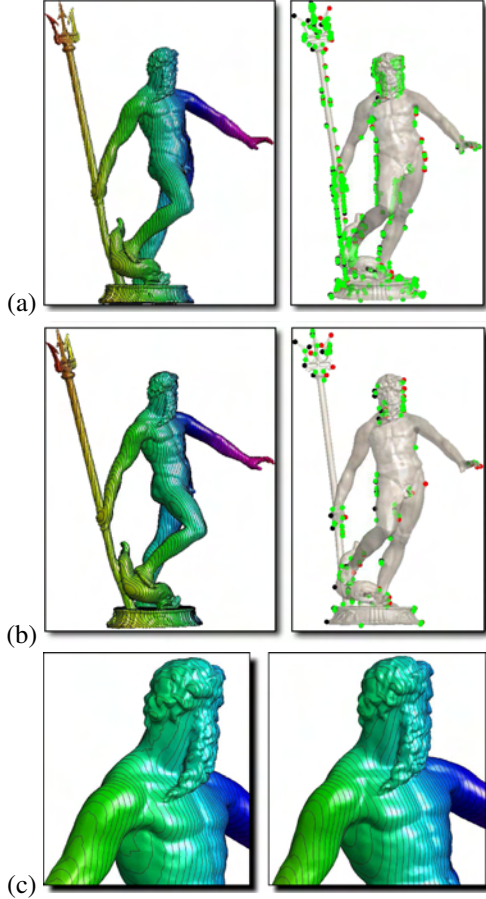


Figure 5: (a) Noisy ($m = 127$, $M = 57$, $s = 188$) and (b) smooth scalar function ($m = 12$, $M = 14$, $s = 30$) achieved applying the Tikhonov regularization. (c) Zoom-in on the level sets of the input (left) and smoothed (right) function.

of triangle areas

$$b_{ij} := \begin{cases} \frac{|t_r| + |t_l|}{12} & (i, j) \text{ edge,} \\ \frac{\sum_{k \in N(i)} |t_k|}{6} & i = j. \end{cases}$$

Here, t_r and t_l are the triangles that share the edge (i, j) , t_k , $k \in N(i)$, is a triangle belonging to the 1-star of the vertex of index i , and $|t_k|$ is the area of the triangle t_k . Since B is positive definite we measure the least-squares error between f and \tilde{f} with respect to the metric induced by B ; i.e.,

$$\|\tilde{\mathbf{f}} - \mathbf{f}\|_B^2 := (\tilde{\mathbf{f}} - \mathbf{f})^T B (\tilde{\mathbf{f}} - \mathbf{f}).$$

In this case, the normal equations of the new functional $\mathcal{F}(\tilde{\mathbf{f}}) := \epsilon \|\tilde{\mathbf{f}} - \mathbf{f}\|_B^2 + \|\tilde{L}\tilde{\mathbf{f}}\|_2^2$ are

$$(L^T L + \epsilon B)\tilde{\mathbf{f}} = \epsilon B \mathbf{f}. \quad (5)$$

The coefficient matrix in (5) is sparse and positive definite; in particular, $\tilde{\mathbf{f}}$ is uniquely defined as solution of the previous linear system (see Figure 6).

The main criterion to choose the identity or the mass matrix as B in (1) is the variation of the triangle areas of the input surface. To show the different results, we consider these two

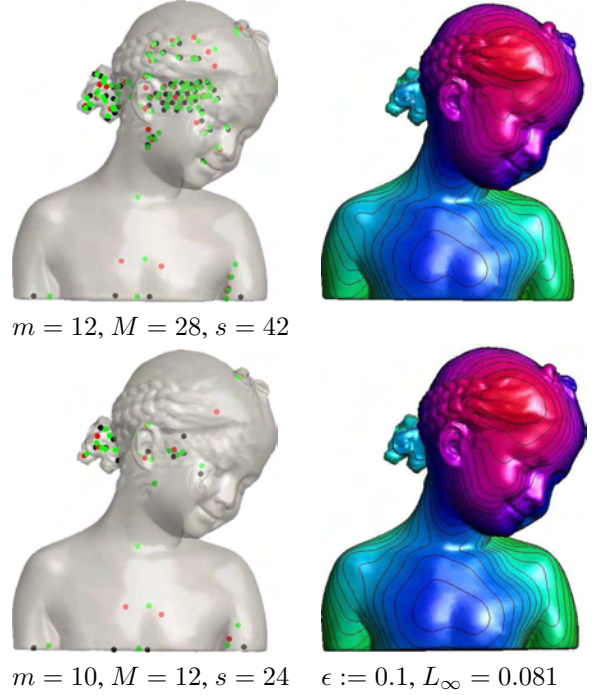


Figure 6: Tikhonov regularization without constraints and achieved using the linear FEM approximation of the Laplacian matrix. The level sets and critical points of the input and smoothed scalar function are shown in the first and second row, respectively.

choices of B and apply the Tikhonov regularization to a noisy scalar function defined on an irregularly-sampled triangle mesh. From the examples in Figure 7 and 8, it follows that using B instead of I is more suitable for surfaces with irregular triangles and provides smooth functions with a low number of critical points. In case of regular sampling, our tests have shown that both choices give similar results.

Error bounds for the smoothed scalar function. Let us suppose that we perturb the f -values and consider the new scalar function $f_e : \mathcal{M} \rightarrow \mathbb{R}$ whose values on the vertices of \mathcal{M} are $f_e := (f(\mathbf{p}_i) + e_i)_{i=1}^n$, with $\mathbf{e} := (e_i)_{i=1}^n$. Then, we denote with \tilde{f} and \tilde{f}_e the solution to the unperturbed and perturbed problem, respectively; the corresponding function values are $\tilde{\mathbf{f}} := (\tilde{f}(\mathbf{p}_i))_{i=1}^n$, $\tilde{\mathbf{f}}_e := (\tilde{f}_e(\mathbf{p}_i))_{i=1}^n$. In the following, we estimate the error $\|\tilde{\mathbf{f}} - \tilde{\mathbf{f}}_e\|_2$ and distinguish two cases on the base of the smoothing techniques that are applied.

If we apply the Tikhonov regularization using the Euclidean norm, $\tilde{\mathbf{f}}$ and $\tilde{\mathbf{f}}_e$ satisfy the normal equations

$$(\Delta^2 + \epsilon I) X^T \tilde{\mathbf{f}} = \epsilon X^T \mathbf{f}, \quad (\Delta^2 + \epsilon I) X^T \tilde{\mathbf{f}}_e = \epsilon X^T \mathbf{f}_e;$$

it follows that

$$\begin{aligned} \|\tilde{\mathbf{f}} - \tilde{\mathbf{f}}_e\|_2 &\leq \|\epsilon X (\Delta^2 + \epsilon I)^{-1} X^T (\mathbf{f} - \mathbf{f}_e)\|_2 \\ &\leq \frac{\epsilon}{\lambda_{\min}(\Delta^2 + \epsilon I)} \|\mathbf{f} - \mathbf{f}_e\|_2 = \|\mathbf{e}\|_2. \end{aligned}$$

To prove the last equality, note that $\lambda_1 = 0$ and therefore $\lambda_{\min}(\Delta^2 + \epsilon I) = \lambda_{\min}^2(\Delta) + \epsilon = \lambda_1^2 + \epsilon = \epsilon$. From the previous inequality, we conclude that for all reasonable parameters ϵ

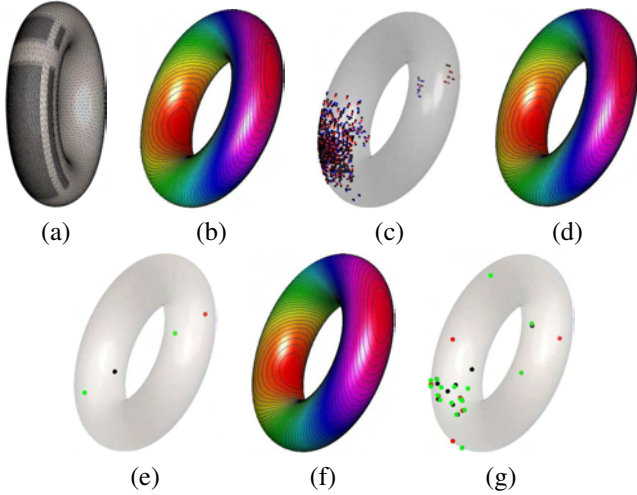


Figure 7: (a) Toroidal surface \mathcal{M} with irregularly sampled patches; (b,c) level sets and critical points of a noisy scalar function ($m = 266$, $M = 258$, $s = 524$) defined on \mathcal{M} . Results achieved by applying the Tikhonov regularization with respect to (d,e) the mass matrix related to the linear FEM discretization of the Laplace-Beltrami operator ($m = 1$, $M = 1$, $s = 2$) and (f,g) the Euclidean norm ($m = 9$, $M = 8$, $s = 17$).

the perturbation bound of the \tilde{f}_e -values is proportional to the magnitude $\|\mathbf{e}\|_2$ of the noise.

If we apply the Tikhonov regularization using the FEM metric, we have that

$$(L^T L + \epsilon B)\tilde{\mathbf{f}} = \epsilon B\mathbf{f}, \quad (L^T L + \epsilon B)\tilde{\mathbf{f}}_e = \epsilon B\mathbf{f}_e;$$

therefore,

$$\begin{aligned} \|\tilde{\mathbf{f}} - \tilde{\mathbf{f}}_e\|_2 &= \|\epsilon(L^T L + \epsilon B)^{-1}B(\mathbf{f} - \mathbf{f}_e)\|_2 \\ &\leq \epsilon\|(L^T L + \epsilon B)^{-1}\|_2\|B\|_2\|\mathbf{e}\|_2 \\ &\leq \epsilon\lambda_{\min}^{-1}(L^T L + \epsilon B)\|B\|_2\|\mathbf{e}\|_2. \end{aligned}$$

We conclude that the perturbation bound is proportional to the trade-off ϵ , the eigenvalue $\lambda_{\min}^{-1}(L^T L + \epsilon B)$, the norm $\|B\|_2$, and the error magnitude $\|\mathbf{e}\|_2$.

In the approximation schemes previously described, as ϵ increases (see Figure 9 and 10), the approximation error dominates the value of the functional \mathcal{F} in (1); therefore, the solution is forced to precisely approximate all the f -values on \mathcal{M} and the error $\|\mathbf{f} - \tilde{\mathbf{f}}\|_2$ is minimized. In particular, the number of critical points of f increases with ϵ . As ϵ tends to zero, the smoothness of \tilde{f} becomes predominant and filters out close critical points and/or f -values. In this case, we have a lower number of critical points and a higher approximation error, which is estimated according to the previous upper bounds. A detailed discussion on the choice of ϵ is presented in [13, 28]. Figure 10 shows the selection of the optimal value of the threshold ϵ , which is based on the L -curve criterion [13] and provides the approximation of f that is the best compromise between accuracy and smoothness.

It is worth noting that these schemes do not take into account the configuration of the critical points of f and are guided by all the f -values at the mesh vertices. Therefore, in Section 4.3

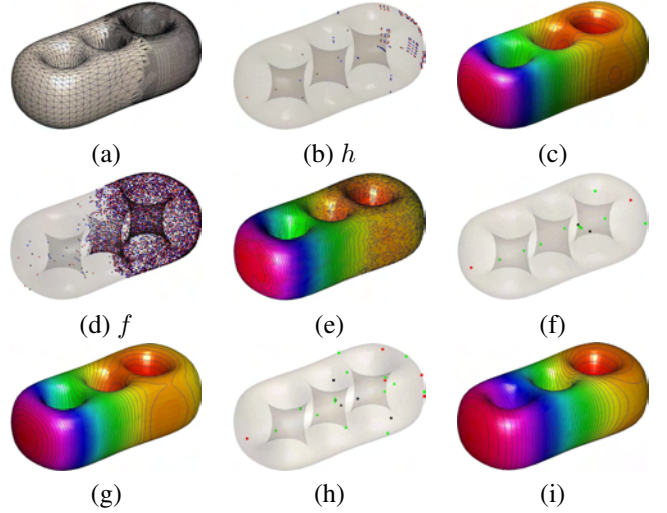


Figure 8: (a) Irregularly-sampled surface \mathcal{M} , (b) critical points ($m = 35$, $M = 35$, $s = 74$) and (c) level sets of a scalar function h defined on \mathcal{M} . (d,e) Noisy version f of h with clustered critical points ($m = 2024$, $M = 1993$, $s = 4021$). Critical points and level sets of the smoothed approximation of f achieved by applying the Tikhonov regularization with respect to (f,g) the mass ($m = 3$, $M = 2$, $s = 9$) and (h,i) identity matrix ($m = 5$, $M = 5$, $s = 14$). Comparing (e) with (g,i) shows that the variation and shape of the level sets is almost the same; however, using an area-dependent metric reduces the number of critical points of the smoothed approximation with respect to both the input (b) and noisy (d) function.

we change (3) in such a way that the solution of the corresponding minimization problem is forced to accurately approximate those f -values that characterize the behavior of f .

4.3. Smoothing scalar functions with constraints on the critical points distribution

In several cases, the critical points of a scalar function $f : \mathcal{M} \rightarrow \mathbb{R}$, defined on a 3D shape \mathcal{M} , are more essential than geometric error to analyze the properties measured of f and \mathcal{M} . For instance, the spectral quadrilateral remeshing [8, 14] is mainly guided by the number and position of the critical points of the Laplacian functions $\{f_i\}_{i=1}^n$. Therefore, smoothing techniques constrained to preserve a subset of the critical points of f_i , while discarding redundant critical points with close positions and function values, provide a flexible control over the number, shape, and size of the resulting quadrangular patches. Removing clustered critical points and filtering small variations of the function values also diminish the number of patches and improves the smoothness of the patch boundaries (see Section 5).

Since traditional approaches to function approximation are mainly driven by a numerical error estimation, they do not provide an error metric useful to assess the preservation of the topological and geometric features of a given scalar function. Our aim is to define an approximation scheme that preserves the topological features of $f : \mathcal{M} \rightarrow \mathbb{R}$ through its critical points, or a subset of them, and distinguishes the global structure of f from its local details. Therefore, we now include in the smoothing process a set of constraints related to the topological features of f that should be maintained.

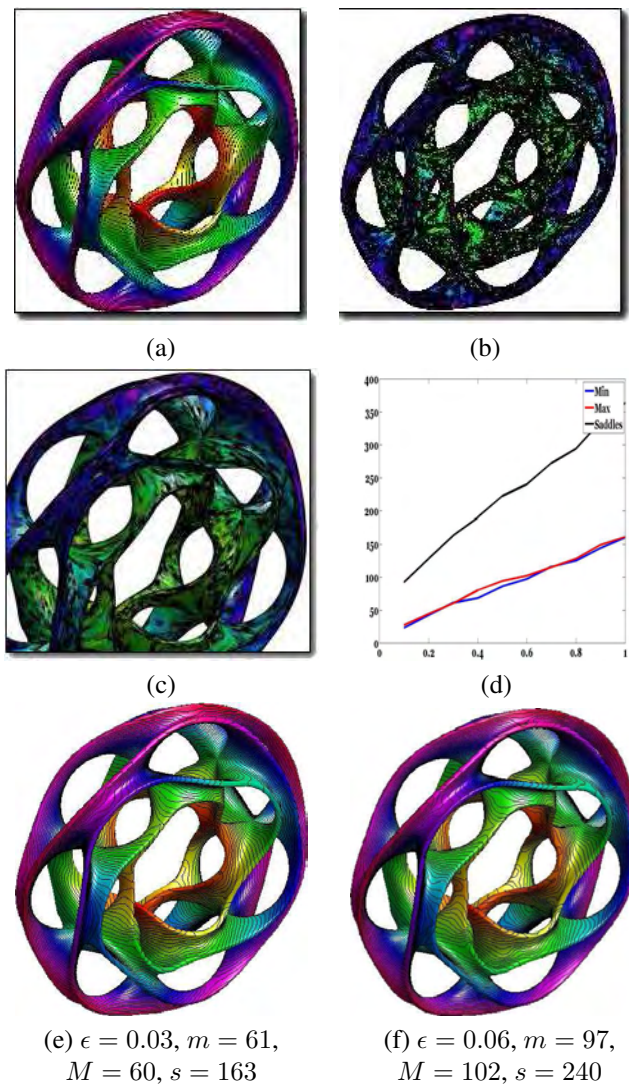


Figure 9: We generated a noise scalar function ($m = 4248, M = 4233, s = 8523$) (b) by adding a Gaussian noise to a smooth map (a) defined on a 22-genus surface. (c) Zoom-in. (d) Results of the Tikhonov regularization with respect to several thresholds ϵ . (e,f) Level sets and number of critical points of two smooth scalar functions corresponding to different values of ϵ .

To this end, we compute a smooth approximation $\tilde{f} : \mathcal{M} \rightarrow \mathbb{R}$ of f that preserves/approximates a subset of the critical points of f . More precisely, let $\{\mathbf{p}_i, i \in \mathcal{C}\}$ be the set of critical points of f or those that have been preserved by the δ -simplification scheme described in Section 3. We remind that setting $\delta = 0$ we use all the critical points of f as constraints. Then, we consider the set

$$\mathcal{I} := \mathcal{C} \cup \{j \in N(i), i \in \mathcal{C}\},$$

whose indices belong to \mathcal{C} and to the corresponding 1-stars $\{N(i), i \in \mathcal{C}\}$. Assuming that the indices in \mathcal{I} are without repetitions and that its cardinality is k , we compute the approximation \tilde{f} of f using the set $\{f(\mathbf{p}_i), i \in \mathcal{I}\}$ as interpolating (see Section 4.3.1) or least-squares constraints (see Section 4.3.2).

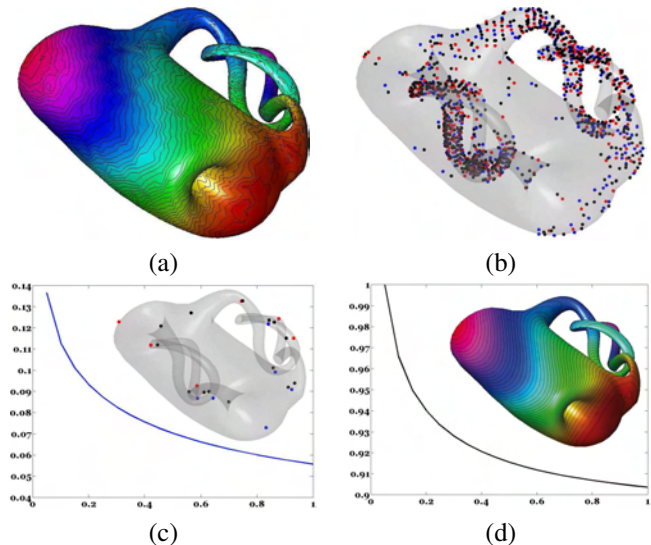


Figure 10: (a) Level sets and (b) critical points of a noisy scalar function f ($m = 312, M = 280, s = 594$). Variation (y -axis) of the (c) L_∞ -approximation error and (d) the Sobolev semi-norm (see Section 4.1) of the Tikhonov approximation of f with respect to several thresholds ϵ (x -axis). The pictures (c,d) also show the function that represents the best compromise between approximation accuracy and smoothness.

4.3.1. Smoothing scalar functions with interpolation constraints

To guarantee that the points of \mathcal{C} are the critical points of a smooth scalar function $\tilde{f} : \mathcal{M} \rightarrow \mathbb{R}$, we define \tilde{f} as the solution of the constrained minimization problem

$$\begin{cases} \min_{\tilde{f} \in \mathbb{R}^n} \|\tilde{L}\tilde{f}\|_2 \\ \tilde{f}(\mathbf{p}_i) := f(\mathbf{p}_i), \quad i \in \mathcal{I}. \end{cases} \quad (6)$$

In this way, we have that the set $\tilde{\mathcal{C}}$ of critical points of \tilde{f} contains the set \mathcal{C} . To compute the solution of the aforementioned problem, we consider the complement \mathcal{I}^C of \mathcal{I} and we note that

$$\begin{aligned} (\tilde{L}\tilde{f})_i &= l_{ii}\tilde{f}(\mathbf{p}_i) - \sum_{j \in N(i)} l_{ij}\tilde{f}(\mathbf{p}_j) = l_{ii}\tilde{f}(\mathbf{p}_i) \\ &- \sum_{j \in N(i) \cap \mathcal{I}^C} l_{ij}\tilde{f}(\mathbf{p}) - \sum_{j \in N(i) \cap \mathcal{I}} l_{ij}f(\mathbf{p}_j), \quad i \in \mathcal{I}^C. \end{aligned}$$

Indicating with $\mathbf{g} := (\tilde{f}(\mathbf{p}))_{i \in \mathcal{I}^C} \in \mathbb{R}^{n-k}$ the set of unknowns, the previous identities can be written in matrix form as $\tilde{L}\mathbf{g} = \mathbf{b}$. Here, $\tilde{L} \in \mathbb{R}^{(n-k) \times (n-k)}$ is the matrix achieved by cancelling the i^{th} -row and i^{th} -column of L , $i \in \mathcal{I}$, and the entries of the constant term $\mathbf{b} \in \mathbb{R}^{n-k}$ are given by $\sum_{j \in N(i) \cap \mathcal{I}} l_{ij}f(\mathbf{p}_j)$, $i \in \mathcal{I}^C$. Therefore, the constrained least-squares minimization problem (6) is equivalent to

$$\min_{\mathbf{x} \in \mathbb{R}^{n-k}} \{\|\tilde{L}\mathbf{x} - \mathbf{b}\|_2\}.$$

Since L is a sparse matrix and $\text{rank}(L) = n - 1$, it follows that \tilde{L} is still sparse and $\text{rank}(\tilde{L}) = n - k$, $k \geq 1$; indeed, the vector \mathbf{g} is uniquely defined by the equation $\tilde{L}\mathbf{g} = \mathbf{b}$. Examples are shown in Figure 11 and 12.

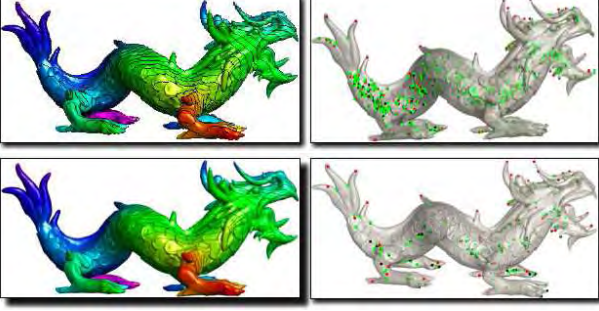


Figure 11: Tikhonov smoothing with interpolating constraints. The level sets and critical points of the input and smoothed scalar function are shown in the first and second row. The L_∞ -error is 0.08.

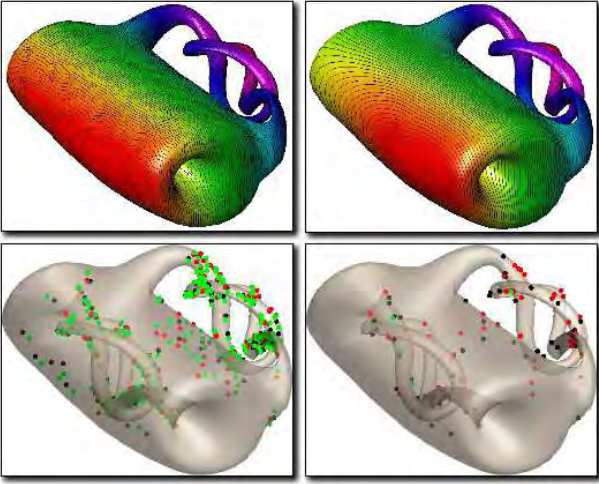


Figure 12: *First row*: level sets of the noisy f (left) and smoothed \tilde{f} (right) scalar function. *Second row*: critical points of (left) f ($M = 18$, $m = 38$, $s = 58$) and (right) simplified set ($M = 10$, $m = 12$, $s = 10$). This last set of critical points are used as interpolating constraints to compute \tilde{f} ($M = 12$, $m = 14$, $s = 28$). See also Figure 14.

4.3.2. Smoothing f with selected least-squares constraints

Let $\mathcal{K} \subseteq \{1, \dots, n\}$ be a set of indices, $(f(\mathbf{p}_i))_{i \in \mathcal{K}}$ the set of f -values that we want to preserve, and $\|L\mathbf{f}\|_2$ the regularization term. Then, the function $\tilde{f} : \mathcal{M} \rightarrow \mathbb{R}$ which is the best compromise between the constraints on the f -values in \mathcal{K} , i.e. $\sum_{i \in \mathcal{K}} |\tilde{f}(\mathbf{p}_i) - f(\mathbf{p}_i)|^2$, and the regularization term is the solution of the following problem

$$\min_{\tilde{\mathbf{f}} \in \mathbb{R}^n} \left\{ \epsilon \sum_{i \in \mathcal{K}} |\tilde{f}(\mathbf{p}_i) - f(\mathbf{p}_i)|^2 + \|L\tilde{\mathbf{f}}\|_2^2 \right\}. \quad (7)$$

Indicating with $\mathcal{F}(\tilde{f}(\mathbf{p}_1), \dots, \tilde{f}(\mathbf{p}_n))$ the functional in (7), we have that the derivative of \mathcal{F} with respect to the unknown $\tilde{f}(\mathbf{p}_k)$ is

$$\begin{cases} \sum_{i,j=1}^n l_{ij} l_{ik} \tilde{f}(\mathbf{p}_j) + \epsilon(\tilde{f}(\mathbf{p}_k) - f(\mathbf{p}_k)) & k \in \mathcal{K}, \\ \sum_{i,j=1}^n l_{ij} l_{ik} \tilde{f}(\mathbf{p}_j) & k \in \mathcal{K}^C. \end{cases}$$

The equations $\nabla \mathcal{F} = \mathbf{0}$ can be written in matrix form as

$$(L^T L + \epsilon \Delta) \tilde{\mathbf{f}} = \epsilon \mathbf{b},$$

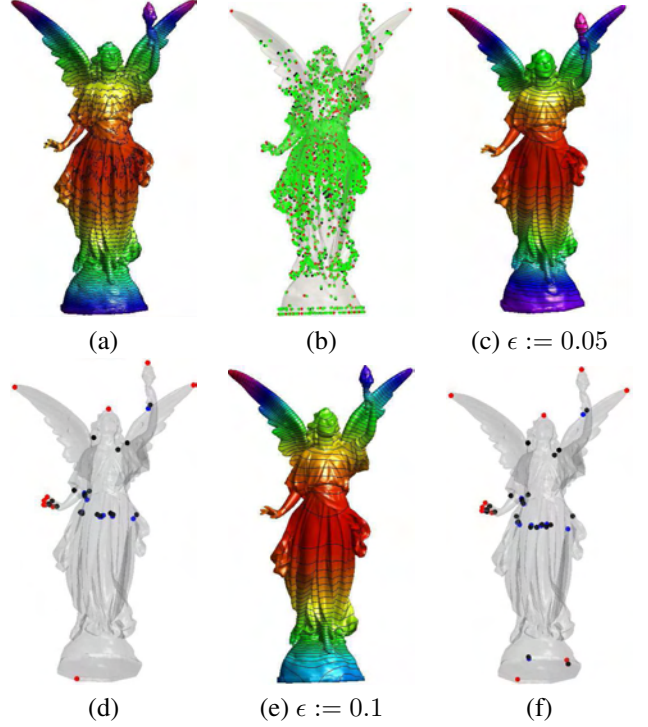


Figure 13: Critical points and level sets of (a,b) a noisy scalar function and (c-g) the smoothed approximations achieved by using different thresholds and all the critical points as least-squares constraints. Statistics are reported in Table 1.

with $\Delta := (\Delta_{ij})_{i,j=1}^n \in \mathbb{R}^{n \times n}$, $\mathbf{b} := (b_i)_{i=1}^n \in \mathbb{R}^n$, and

$$\Delta_{ij} := \begin{cases} 1 & i = j \in \mathcal{K}, \\ 0 & \text{else,} \end{cases} \quad b_i := \begin{cases} f(\mathbf{p}_i) & i \in \mathcal{K}, \\ 0 & i \in \mathcal{K}^C. \end{cases}$$

Similarly to the discussion in Section 4.2, it is possible to prove that the coefficient matrix $L^T L + \epsilon \Delta$, $\epsilon > 0$, is symmetric, sparse, and positive definite. While in (2) all the f -values have been used to measure the least-squares error $\|\mathbf{f} - \tilde{\mathbf{f}}\|_2$, in (7) this discrepancy is measured only on the set $\{\mathbf{p}_i, i \in \mathcal{K}\}$ of feature points of f (see Figure 13, 14, and Table 1).

In our tests, we have selected \mathcal{K} as the set of all the critical points of f (see Figure 15(a)) or the points preserved by the δ -simplification (see Figure 15(b)); in both cases, we can also consider the points of the corresponding 1-stars (i.e., the set \mathcal{I} introduced in the previous section). The best compromise between smoothness, number of critical points, and approximation error is achieved by considering all the critical points of f and the vertices of the corresponding 1-stars as least-squares constraints. Infact, close critical points and f -values are filtered out by the regularization term in (7), while guaranteeing that the new function values smoothly vary in these regions without being constant on the edges and faces of \mathcal{M} . Here, the interpretation of the threshold ϵ resembles the discussion in Section 4.2. Whenever it is important to have a higher approximation accuracy and smoothness in those regions that include the critical points of f (see Figure 15), we prefer the least-squares constraints to the Tikhonov regularization.

Table 1: With reference to Figure 13, the table shows the L_∞ -approximation error and the number of critical points (m, M, s) of the smooth approximation of a noisy scalar function achieved using different thresholds ϵ .

Figure	ϵ	m	M	s	L_∞
Fig. 13(a,b)	–	1398	1438	2834	0.0
–	0.01	13	5	16	0.121
–	0.02	23	12	33	0.092
–	0.03	12	14	24	0.104
–	0.04	11	10	19	0.128
Fig. 13(c,d)	0.05	12	10	20	0.127
–	0.06	18	10	26	0.116
–	0.07	15	10	23	0.112
–	0.08	14	10	22	0.115
–	0.09	14	10	22	0.123
Fig. 13(e,f)	1.0	15	11	24	0.127

Error bounds for the smoothed scalar functions. If we apply the smoothing with interpolation constraints, then $\tilde{\mathbf{f}}$ and $\tilde{\mathbf{f}}_e$ assume the same values $\{f(\mathbf{p}_i)\}_{i \in \mathcal{I}}$ on the set of constrained points $\{\mathbf{p}_i\}_{i \in \mathcal{I}}$; therefore, on these points the error $|\tilde{f}(\mathbf{p}_i) - \tilde{f}_e(\mathbf{p}_i)|$, $i \in \mathcal{I}$, is null. On the vertices $\{\mathbf{p}_i\}_{i \in \mathcal{I}^c}$, the values $(\tilde{f}(\mathbf{p}_i))_{i \in \mathcal{I}^c}$ and $(\tilde{f}_e(\mathbf{p}_i))_{i \in \mathcal{I}^c}$ satisfy the normal equations

$$\tilde{L}(\tilde{f}(\mathbf{p}_i))_{i \in \mathcal{I}^c} = \mathbf{b} \quad \text{and} \quad \tilde{L}(\tilde{f}_e(\mathbf{p}_i))_{i \in \mathcal{I}^c} = \tilde{\mathbf{b}},$$

with \tilde{L} submatrix of the Laplacian matrix. Hence,

$$\begin{aligned} \|\mathbf{f} - \mathbf{f}_e\|_2 &= \|(\tilde{f}(\mathbf{p}_i))_{i \in \mathcal{I}^c} - (\tilde{f}_e(\mathbf{p}_i))_{i \in \mathcal{I}^c}\|_2 \\ &\leq \|\tilde{L}^{-1}(\mathbf{b} - \tilde{\mathbf{b}})\|_2 \leq \|\tilde{L}^{-1}\|_2 \|\mathbf{b} - \tilde{\mathbf{b}}\|_2 \\ &\leq \lambda_{\min}^{-1}(\tilde{L}) \|\mathbf{b} - \tilde{\mathbf{b}}\|_2. \end{aligned}$$

We conclude that the perturbation bound related to the function values on the unconstrained vertices $\{\mathbf{p}_i\}_{i \in \mathcal{I}}$ is proportional to $\lambda_{\min}^{-1}(\tilde{L})$ and to the perturbation $\|\mathbf{b} - \tilde{\mathbf{b}}\|_2$ related to the right-hand side.

If we apply the smoothing with least-squares constraints, then $\tilde{\mathbf{f}}$ and $\tilde{\mathbf{f}}_e$ are the solution of the following linear systems

$$\begin{cases} (L^T L + \epsilon \Delta) \mathbf{f} = \mathbf{b}, \\ (L^T L + \epsilon \Delta) \mathbf{f}_e = \mathbf{b} + \epsilon \mathbf{e}. \end{cases}$$

Therefore, we get the inequality

$$\|\tilde{\mathbf{f}} - \tilde{\mathbf{f}}_e\|_2 = \|\epsilon(L^T L + \epsilon \Delta)^{-1} \mathbf{e}\|_2 \leq \epsilon \lambda_{\min}^{-1}(L^T L + \epsilon \Delta) \|\mathbf{e}\|_2.$$

It follows that the perturbation bound related to the function values is proportional to the threshold ϵ , the perturbation error $\|\mathbf{e}\|_2$, and the eigenvalue $\lambda_{\min}^{-1}(L^T L + \epsilon \Delta)$.

5. Discussion

Since the choice of the parameter ϵ and of the set of constrained points has been already discussed in those sections where each method has been presented, in the following we

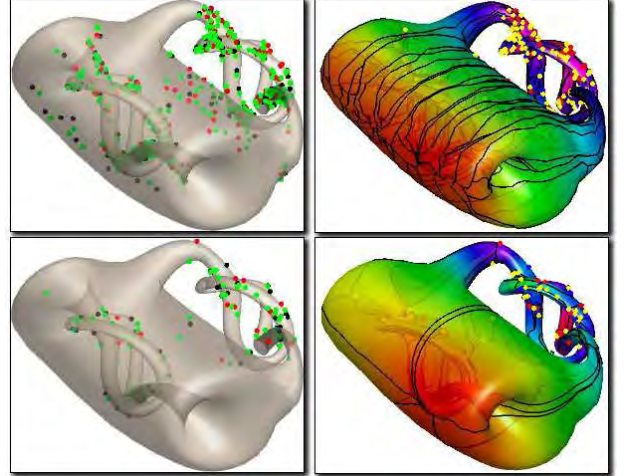


Figure 14: *First row:* critical points and Morse complex of a noisy scalar function f ($M = 18, m = 38, s = 58$). *Second row:* critical points of the scalar function \tilde{f} ($m = 10, M = 12, s = 24$) achieved by smoothing f with least-squares constraints on the set of preserved critical points shown in (a,right corner).

Table 2: Computation cost of the smoothing techniques discussed in the paper; here, n is the number of vertices of the input triangle mesh and k is the number of anchor points.

Method	Eq.	Computational Cost
<i>Critical points simpl.</i>	–	$O(n)$
<i>Tikh. $B := I$</i>	(1)	$O(n \log n)$
<i>Tikh. B mass matrix</i>	(1)	$O(n \log n)$
<i>Tikh. interp. constr.</i>	(6)	$O((n - k) \log(n - k))$
<i>Tikh. least-squares constr.</i>	(7)	$O(n \log n)$

focus our attention on the applications, computational cost, and comparison of our approach with previous work.

In [8, 14], the Morse-Smale complexes of the Laplacian eigenfunctions $\{f_i\}_{i=1}^n$ and the iso-lines of the global multi-chart parameterization have been used to automatically create a quadrangular remeshing of 3D surfaces. For both methods, the smoothness of each function f_i , used to guide the remeshing and the control over the number and position of its critical points, is crucial. Infact, the number and location of the critical points determine the vertices, dimension, and alignment of the quadrangular patches. Furthermore, the Laplacian eigenfunctions have increasing numbers of critical points at progressively higher frequencies and numerical instabilities might result in clusters of critical points with close positions and f_i -values. In all these cases, our approach addresses the previous problems in one step by cancelling extraneous critical points, removing small and noisy arcs of the Morse complex through the smoothing of the f_i -values, and constraining the regularization to preserve the critical points with high persistency values. Examples of regularized Morse complexes with a low number of critical points and smooth paths among them are shown in Figure 4(f,g) and 14.

As already mentioned in Section 1, previous work is not able

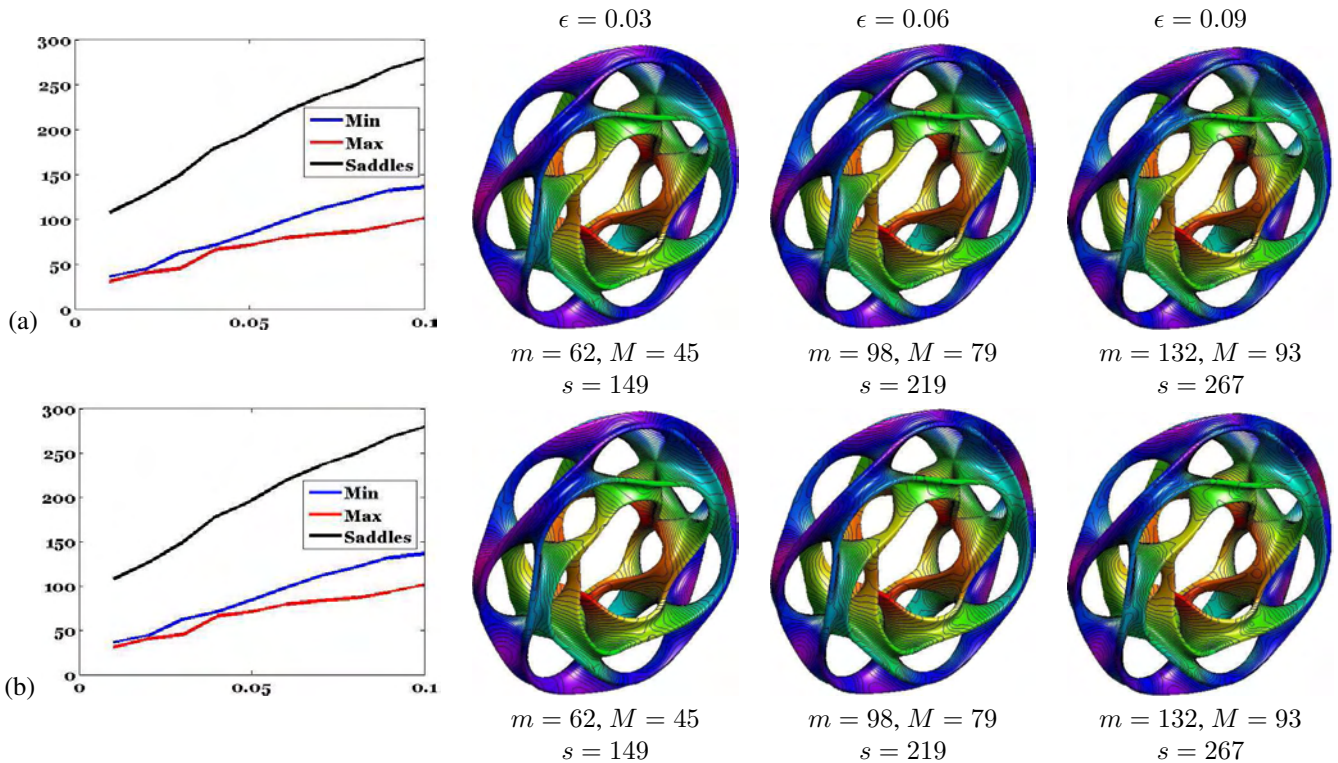


Figure 15: With reference to Figure 9, level sets of three representative smooth functions achieved by applying the least-squares regularization constrained to (a) all and (b) the δ -simplified critical points ($\delta := 0.2$). The evolution of the number of critical points (y -axis) with respect to several thresholds ϵ (x -axis) is shown in the first column. In both cases, the results is almost the same. Here, the variation of the number of critical points is lower than the example in Figure 9.

to constrain the critical points during the smoothing process. As shown in Figure 16, the Tikhonov regularization also provides smoother results than [15]. Infact, the number of parameters used by the saliency-driven filtering do not make explicit the magnitude of the final smoothing. Finally, the proposed variants of the Tikhonov regularization combine two types of smoothing effects: one is introduced by the least-squares approximation term and the second one is provided by the smoothing properties of the Laplacian matrix.

Table 2 summarizes the computational cost of the different variants of the proposed smoothing framework. Since their cost is almost $O(n \log n)$, with n number of vertices of \mathcal{M} , these methods are competitive with previous work, whose cost varies from $O(n)$ [24] to $O(n \log n)$ [15].

6. Future work

This paper has presented a framework to smooth a scalar function f with or without constraints on the preservation of the feature points of f (see Figure 17). These features are identified through a δ -simplification of the critical points of f . The unconstrained smoothing is usually applied when the input scalar function has several and close critical points with a low persistency of the corresponding f -values. Smoothing f with interpolating or least-squares constraints is preferable in all those applications, such as quadrilateral remeshing and skeleton extraction, where a direct control on the final number and position of the critical points is crucial. In this case, the inter-

polating or least-squares constraints are chosen on the base of the application needs. The threshold δ used for the simplification of the critical points can be easily selected on the base of the variation of the f -values. To select the tradeoff ϵ between smoothness and approximation accuracy, statistical and heuristic methods (e.g., L -curve, best ration criterion) have been extensively discussed in [13, 28]. The proposed approach can be applied to all those applications where the critical points have a specific meaning. Infact, in these cases critical points must be preserved, relocated, or cancelled according to specific rules which guarantee a correct surface tessellation (e.g., quadrilateral remeshing) and skeletonization, molecular simulation and interaction (e.g., docking). As future work, we plan to generalize the proposed scheme to multi-dimensional data and arbitrary basis functions.

Acknowledgments

This work has been partially supported by the FOCUS K3D Coordination Action and the Italy-Israel project SHALOM. Special thanks are given to Michela Spagnuolo for helpful discussions on discrete Morse theory and the reviewers for their precious comments, which helped us to improve the content of the paper. Models are courtesy of the AIM@SHAPE repository, the Stanford 3D Scanning Repository, Carlo Sequin (University of Berkely), Tao Ju and Cindy Grimm (Washington University in St. Louis).

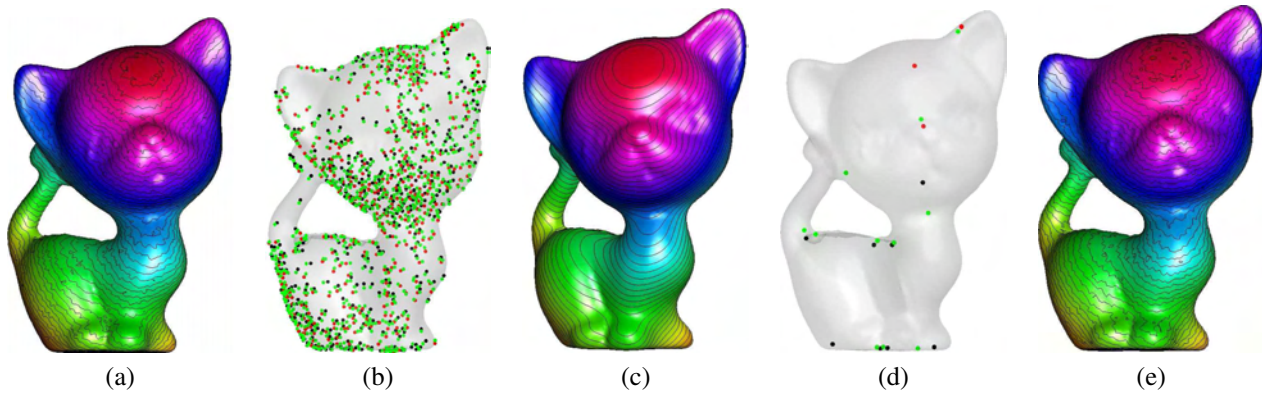


Figure 16: Level sets and critical points of (a,b) a noisy ($m = 416$, $M = 382$, $s = 798$) and a smoothed scalar function computed (c,d) using the Tikhonov regularization with respect to the mass matrix of the linear FEM discretization of the Laplace-Beltrami operator and (e) the saliency smoothing [15]. In (d), the smoothed scalar function has $m = 7$ minima, $M = 2$ maxima, and $s = 9$ critical points.

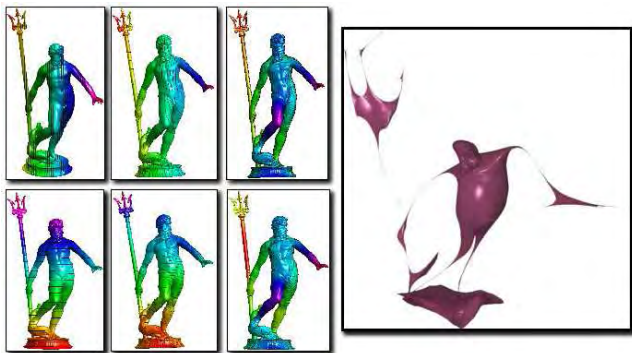


Figure 17: Given the height functions f_x , f_y , and f_z on \mathcal{M} with respect to the coordinates axis (top row), we visualize the corresponding approximations \tilde{f}_x , \tilde{f}_y (interpolating constraints), and \tilde{f}_z (bottom row) as an approximation \mathcal{Q} of \mathcal{M} . The smoothness of \mathcal{Q} confirms that the approximation scheme generates smooth scalar functions. A larger discrepancy between \mathcal{M} and \mathcal{Q} highlights a larger error between the input and the approximated scalar functions.

References

[1] N. Aronszajn. Theory of reproducing kernels. *Transactions of the American Mathematical Society*, 68:337–404, 1950.

[2] T. Banchoff. Critical points and curvature for embedded polyhedra. *Journal of Differential Geometry*, 1:245–256, 1967.

[3] M. Belkin and P. Niyogi. Laplacian eigenmaps for dimensionality reduction and data representation. *Neural Computations*, 15(6):1373–1396, 2003.

[4] M. Bertero. *Regularization methods for linear inverse problems*. Inverse Problems, Springer-Verlag, Berlin, 1986.

[5] S. Biasotti, B. Falcidieno, L. De Floriani, P. Frosini, D. Giorgi, C. Landi, L. Papaleo, and M. Spagnuolo. Describing shapes by geometric-topological properties of real functions. *ACM Computing Surveys*, 40(4).

[6] P.-T. Bremer, H. Edelsbrunner, B. Hamann, and V. Pascucci. A topological hierarchy for functions on triangulated surfaces. *IEEE Transactions on Visualization and Computer Graphics*, 10(4):385–396, 2004.

[7] M. Desbrun, M. Meyer, P. Schröder, and A. H. Barr. Implicit fairing of irregular meshes using diffusion and curvature flow. In *ACM Siggraph*, pages 317–324, 1999.

[8] S. Dong, P.-T. Bremer, M. Garland, V. Pascucci, and J. C. Hart. Spectral surface quadrangulation. *ACM Siggraph*, pages 1057–1066, 2006.

[9] H. Edelsbrunner, J. Harer, V. Natarajan, and V. Pascucci. Local and global comparison of continuous functions. In *IEEE Visualization*, pages 275–280, 2004.

[10] H. Edelsbrunner, D. Morozov, and V. Pascucci. Persistence-sensitive sim-

plification functions on 2-manifolds. In *Proc. of the Symposium on Computational Geometry*, pages 127–134, 2006.

[11] M. S. Floater. Analysis of curve reconstruction by meshless parameterization. *Numerical Algorithms*, (32):87–98, 2003.

[12] G. Golub and G.F. VanLoan. *Matrix Computations*. John Hopkins University Press, 2nd. edition, 1989.

[13] P. C. Hansen and D. P. O’Leary. The use of the l-curve in the regularization of discrete ill-posed problems. *SIAM Journal of Scientific Computing*, 14(6):1487–1503, 1993.

[14] J. Huang, M. Zhang, J. Ma, X. Liu, L. Kobbelt, and H. Bao. Spectral quadrangulation with orientation and alignment control. *ACM Transactions on Graphics*, 27(5):1–9, 2008.

[15] Y.-S. Liu, M. Liu, D. Kihara, and K. Ramani. Salient critical points for meshes. In *Proc. of Symposium on Solid and Physical Modeling*, pages 277–282, 2007.

[16] J. Milnor. *Morse Theory*, volume 51 of *Annals of mathematics studies*. Princeton University Press, 1963.

[17] V. Natarajan, Y. Wang, P.-T. Bremer, V. Pascucci, and B. Hamann. Segmenting molecular surfaces. *Computer Aided Geometric Design*, 23(6):495–509, 2006.

[18] X. Ni, M. Garland, and J. C. Hart. Fair Morse functions for extracting the topological structure of a surface mesh. In *ACM Siggraph*, pages 613–622, 2004.

[19] U. Pinkall and K. Polthier. Computing discrete minimal surfaces and their conjugates. *Experimental Mathematics*, 2(1):15–36, 1993.

[20] M. Reuter, F.-E. Wolter, and N. Peinecke. Laplace-Beltrami spectra as Shape-DNA of surfaces and solids. *Computer-Aided Design*, 38(4):342–366, 2006.

[21] O. Sorkine. Differential representations for mesh processing. *Computer Graphics Forum*, 25(4):789–807, 2006.

[22] O. Sorkine, D. Cohen-Or, D. Irony, and S. Toledo. Geometry-aware bases for shape approximation. *IEEE Transactions on Visualization and Computer Graphics*, 11(2):171–180, 2005.

[23] O. Sorkine, Y. Lipman, D. Cohen-Or, M. Alexa, C. Roessl, and H.-P. Seidel. Laplacian surface editing. In *Proc. of the Symposium on Geometry Processing*, pages 179–188, 2004.

[24] G. Taubin. A signal processing approach to fair surface design. In *ACM Siggraph*, pages 351–358, 1995.

[25] G. Taubin. 3D Geometry Compression and Progressive Transmission. In *Eurographics 1999*, 1999.

[26] A.N. Tikhonov and V.Y. Arsenin. *Solutions of Ill-posed Problems*. W.H. Winston Washington, D.C., 1977.

[27] B. Vallet and B. Levy. Spectral geometry processing with manifold harmonics. *Computer Graphics Forum (Eurographics)* 27(2), 2008.

[28] G. Wahba. *Spline Models for Observational Data*, volume 59. SIAM, Philadelphia, 1990.

[29] H. Zhang, O. van Kaick, and R. Dyer. Spectral methods for mesh processing and analysis. In *Eurographics 2007 State-of-the-art Report*, pages 1–22, 2007.